Functional Materials 11, No.1 (2004)

EPR spectroscopy of irradiated bioactive glasses

B.Padlyak, S.Szarska*

Department of Physics, Academy of Bydgoszcz,
11 Weyssenhoff Sq., 85-072 Bydgoszcz, Poland
*Institute of Physics, Wroclaw University of Technology,
27 Wyspianskiego Str., 50-370 Wroclaw, Poland

The X-band ($\nu \cong 9.4$ GHz) EPR spectra of the UV-, X-, and γ-irradiated biologically active glass (Bioglass) samples of two different compositions have been investigated at 77 and 300 K. The generation efficiency of the electron and hole centers depends strongly on the basic Bioglass composition and is almost independent of ionizing radiation type and presence of the non-controlled Fe^{3+} impurity in the glass structure. Influence of pre-treatment in NaCl solution and simulated body fluid on formation processes of the radiation-induced paramagnetic defects in Bioglass have been investigated. Spin Hamiltonian parameters and thermal stability of the radiation-induced centers have been evaluated. Electron structure, formation peculiarities and possible models of the radiation-induced paramagnetic centers in the Bioglass structure are discussed.

Исследованы ЭПР-спектры в X-диапазоне ($\nu \cong 9.4$ ГГц) при температурах 77 и 300 K биологически активных (биологических) стекол двух разных составов, облученных УФ, рентгеновскими и γ-лучами. Эффективность генерации центров электронного и дырочного типа существенно зависит от основного состава биологического стекла и почти не зависит от вида ионизирующей радиации и присутствия неконтролируемой примеси Fe^{3+} в структуре стекла. Исследовано также влияние предварительной обработки в растворах NaCl и модельной физиологической жидкости на процессы формирования радиационных парамагнитных дефектов в биологически активных стеклах. Определены параметры спин-гамильтониана и термическая стабильность радиационных центров. Обсуждаются электронная структура, особенности формирования и возможные модели радиационных парамагнитных центров в структуре биологического стекла.

The alkali-silicate-phosphate glasses of the SiO_2–Na_2O–CaO–P_2O_5 system are intended to be used in the human body as an implant material and become attached to living tissue. Such glasses which contain less than about 60 mass. % SiO_2 are called bioactive. Chemical composition of the bioactive glasses is similar to that of the bones. A bone consists in 1/3 of organic materials and in 2/3 of inorganic materials and water. The inorganic part of the bone consists of calcium phosphate (crystalline hydroxyapatite (HAP) and non-crystalline calcium orthophosphate), calcium carbonate and a small amount of magnesium oxide. Since discovery of the Bioglass [1], various kinds of glasses and glass-ceramics [2–4] have been found to bond to living bone. The Bioglass surface, which can induce the formation of an apatite layer *in vivo*, or is pre-coated with an apatite layer, will demonstrate good bone-bonding properties [5–7].

Electron paramagnetic resonance (EPR) proves to be a powerful tool for studying in different bioactive materials, particularly in the Bioglass. Impurity ions of transition metals and/or radiation-induced electron and hole centers trapped at different sites of the glass network can be used as paramagnetic probes for such studies. At present, impurity paramagnetic ions and radiation-induced defects are widely studied in phosphate glasses of different composition. In particular, the EPR spectrum of radiation-induced PO_4^{2-} hole centers in alkali and

alkali earth phosphate glasses, characterized by hyperfine doublet from ^{31}P isotope (nuclear spin $I = 1/2$) were studied by a number of authors [8–10]. Different models have been proposed for the symmetry of the PO_4^{2-} radical (anisotropy of the g tensor) and localization of unpaired spin in the glass structure. Several papers report about EPR study of the radiation-induced defects in hydroxyapatites [11–14]. Particularly, in the carbonated HAP, F^+ centers were observed [13]. In the plasma-sprayed and β- and γ-irradiated HAP, the anisotropic EPR signal related to the O^- anion-radicals adjacent to a calcium vacancy was observed [14].

In our first paper [15], four types of radiation-induced centers in the Bioglass network were registered using EPR technique, but the nature and structure of some centers were not clearly established up to now. The aim of this work is to study further the nature, structure and formation processes of the radiation-induced paramagnetic defects in the UV-, X- and γ-irradiated Bioglass on the basis of observed EPR spectra analysis and literature data consideration.

Two types of Bioglass were investigated produced by Jelenia Gora Optical Factory (Poland). The glasses have the following, slightly different composition (per cent mass): (1) 45 SiO_2 : 24.5 Na_2O : 24.5 CaO : 6 P_2O_5 (Bioglass^R I or BG I, in literature — 45S5 [1]); and (2) 46 SiO_2 : 25.5 Na_2O : 24.5 CaO : $4P_2O_5$ (Bioglass^R II or BG II). The as-synthesized Bioglass samples were submitted to treatment by the following physiological solutions: 0.9 % NaCl and SBF (simulated body fluid) with pH = 7.4 for 2 h. The SBF contains inorganic ions in concentrations close to those in blood plasma [4, 16]. As was verified by scanning electron microscopy (SEM) and EDAX spectra [17] in areas enriched in calcium and poor in silica are formed in Bioglass samples when exposed to 0.9 % NaCl solution. The comparison of BG I and BG II SEM photograph shows that the formation of hydroxyapatite layer proceeds more fast in BG II. The quite different image shows sample dissolution in SBF: no cracks, surfaces are homogenous, that could suggest that an early stage of HAP formation takes place.

The Bioglass samples for EPR investigation were cut out in approximate size of 8×3×2 mm^3. The samples were UV-irradiated at room temperature using a DKsEL-2000 lamp (power P = 2000 W). The X-irradiation was carried out at room temperature

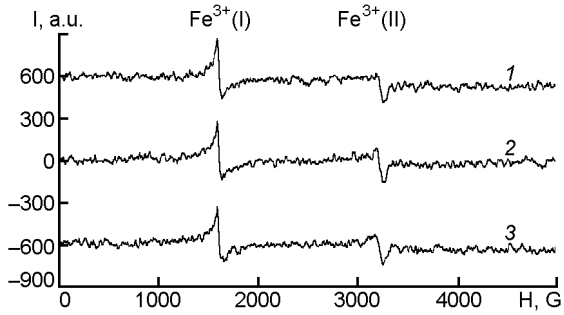

Fig. 1. X-band EPR spectra of non-irradiated Bioglass I at T = 300 K for as-synthesized (*1*), pre-treated in the NaCl solution (*2*), and SBF (*3*) samples.

using an URS-55A standard apparatus (Cu K_α radiation, U = 40 kV, I = 10 mA). The exposure duration was 60 min for both irradiation types. The γ-irradiation of the samples was performed using a ^{90}Sr 40 mCi source. The γ-irradiation dose was 2 Gy. For EPR investigations of the as-synthesized, pre-treated in NaCl solution and SBF, and irradiated Bioglass samples, special quartz tubes of high chemical purity were used.

The X-band EPR spectra were registered at 300 and 77 K using a RADIOPAN SE/X-2544 (Poznan, Poland) and AE-4700 (L'viv, Ukraine) modified computer-controlled commercial spectrometers with cylindrical TM_{110} cavity, operating in the high-frequency (100 kHz) magnetic field modulation mode. The microwave frequency in each case was controlled by means of diphenylpicrylhydrazyl (DPPH) g-marker ($g = 2.0036 \pm 0.0001$). The parameters of EPR spectra were evaluated using a BRUKER computer simulation program "SimFonia". The intensities of EPR lines were evaluated using a special spin standard (number of spins $N_S = 5 \cdot 10^{15}$ spins/G).

It is to note first of all that all the investigated Bioglass samples yield the isotropic EPR signals at $g_{eff} = 4.29$ and $g_{eff} = 2.00$ (Fig. 1). The observed signals are typical of vitreous (or glassy) state [18–22] and were assigned to isolated Fe^{3+} ($3d^5$, $^6S_{5/2}$) ions in octahedral and tetrahedral sites with strong rhombic distortion (Fe^{3+} (I) centers, g_{eff} = 4.29) and in octahedral sites of nearly cubic symmetry (Fe^{3+} (II) centers, g_{eff} = 2.00). Intensity of the Fe^{3+} EPR signals in BG I samples is independent of treatment in NaCl solution and SBF (Fig. 1). Total amount of Fe^{3+} ions in the BG I samples estimated by EPR is 5 to 10 times greater than that in BG II ones and does not exceed 10^{-2} mass. %.

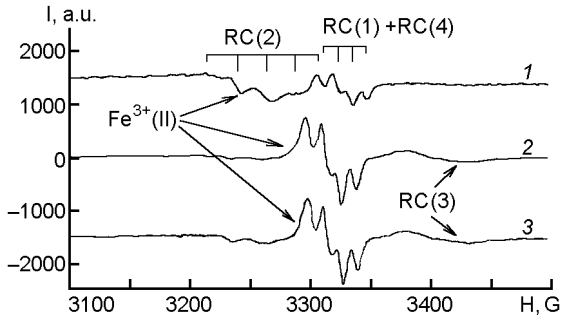

Fig. 2. X-band EPR spectra of UV-irradiated Bioglass I at $T = 300$ K for as-synthesized (*1*), pre-treated in the NaCl solution (*2*) and SBF (*3*) samples.

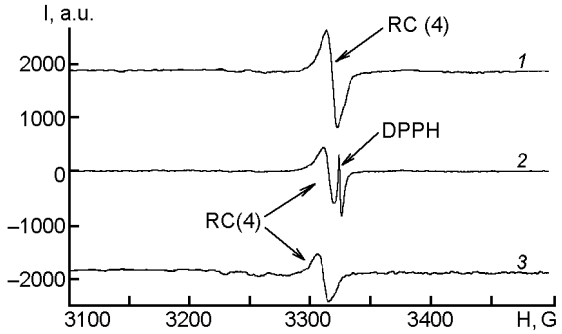

Fig. 3. X-band EPR spectra of Bioglass II at $T = 300$ K for pre-treated in the SBF and UV-irradiated (*1*), as-synthesized and X-irradiated (*2*), pre-treated in the NaCl solution and X-irradiated (*3*) samples.

The UV-, X-, and γ-irradiation of BG I samples at $T = 300$ K results generation of stable radiation-induced centers (RC) of three types denoted as RC (1), RC (2), and RC (3) Fig. 2). The same irradiation of BG II samples generates stable centers of one type, RC (4), in general (Fig. 3). The EPR spectra analysis shows that the RC (4) signals were observed also in the BG I samples as a background of the RC (1) signal (Fig. 2) and the weak RC (2) and RC (3) EPR signals were observed also in BG II samples (Fig. 3). Thus, the generation efficiency of the different paramagnetic centers depends heavily on the basic glass composition. Particularly, a small increase of SiO_2 and Na_2O content and a decrease of P_2O_5 content in the glass composition results in increasing amount of the RC (4) and in a strong decrease of the amount of RC (1), RC (2), and RC (3), and *vice versa*. As a result, the RC (4) signal dominates in BG II samples, whereas the RC (1), RC (2), and RC (3) signals dominate in BG I ones (Figs. 2 and 3). Pre-treatment of the BG I sample in the NaCl solution and SBF results in a decreased amount of RC (2) and an increased amount of RC (3), whereas the amount and type of radiation-induced centers in the BG II are essentially independent of the sample pre-treatment (Figs. 2 and 3). The types of paramagnetic radiation-induced defects in BG I and BG II samples are independent of the kind of ionizing radiation (UV, X, and γ). Also the intensity of EPR spectra of the Fe^{3+} (I) and Fe^{3+} (II) impurity centers in the irradiated BG I and BG II samples remains the same.

The EPR spectrum of RC (1) is characterized by effective g value of the hole type ($g_{eff} > g_e = 2.0023$) and consists of four equidistant lines equal in intensity (Fig. 2). The RC (1) signal could be explained assuming the hyperfine (HF) interaction of unpaired electron of the spin $S = 1/2$ with the magnetic moment of one nearest nucleus with spin $I = 3/2$. Analysis of the isotopic composition of elements occurring in Bioglass shows that the source of HF interaction can be a single nucleus of the ^{23}Na isotope ($I = 3/2$, natural abundance — 100 %).

The RC (2) EPR spectrum is characterized by approximately isotopic hole-like g-factor and consists of five approximately equidistant lines of the intensity ratio close to 1:4:6:4:1, which can be ascribed to ^{31}P isotope ($I = 1/2$, natural abundance — 100 %) superhyperfine structure (SHF). Since the number of components in the SHF structure $N = (2nI + 1) = 5$, the number of equivalent ^{31}P nuclei can be $n = 4$. Thus, the fivefold SHF splitting of the RC (2) EPR signal is caused by interaction of an unpaired electron spin with four nearest nuclei of the ^{31}P isotope.

The EPR spectrum of RC (3) is characterized by an unresolved broad ($\Delta H_{pp} \cong 50$ G) signal with g-factor of the electron type ($g_{eff} < g_e = 2.0023$). The EPR spectrum of RC (4) consists of asymmetric line ($\Delta H_{pp} \cong 9$ G) with a hole-like g-factor of the same value as for RC (1). All observed EPR spectra of the radiation-induced centers in the BG I and BG II samples are temperature independent within the 77 to 300 K range.

Presence of the four different types of radiation-induced paramagnetic centers in the Bioglass network is demonstrated clearly by isochronal annealing of the X-irradiated samples (Figs. 4 and 5). The intensity of EPR signal related to the RC (1) decreases monotonously with increasing annealing temperature and disappears completely at $T \cong 500$ K, whereas the intensity

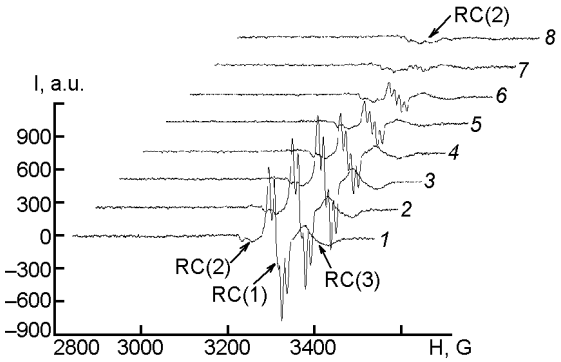

Fig. 4. EPR spectra at T = 300 K in as-synthesized and X-irradiated BG I sample after isochronal (20 min) annealing in air at temperatures (K): 325 (*1*), 375 (*2*), 400 (*3*), 425 (*4*), 450 (*5*), 475 (*6*), 500 (*7*), and 550 (*8*).

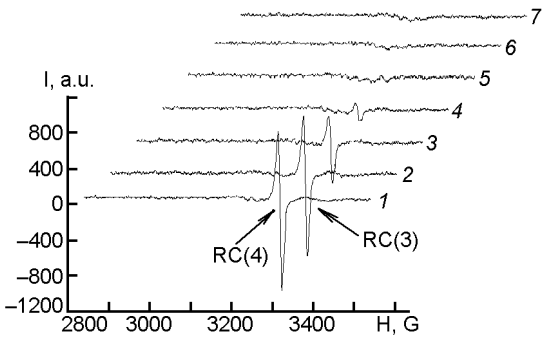

Fig. 5. EPR spectra at T = 300 K in the pretreated in NaCl solution and X-irradiated BG II sample after isochronal (20 min) annealing in air at temperatures (K): 325 (*1*), 375 (*2*), 400 (*3*), 425 (*4*), 450 (*5*), 475 (*6*), and 500 (*7*).

of RC (2) EPR signal remains unchanged even after heating up to $T > 550$ K (Fig. 4). Intensities of EPR signals related to RC (3) and RC (4) decrease monotonously during isochronal annealing (Figs. 4 and 5). As a result, the EPR signal related to RC (3) disappears at $T \cong 550$ K (Figs. 4), whereas the RC (4) related line completely disappears at $T \cong 475$ K (Fig. 5). Thermal stability characteristics of radiation-induced centers in Bioglass are presented in the Table.

The EPR spectra of the observed radiation-induced centers can be described by spin Hamiltonian in the following general form:

$$H = \beta \boldsymbol{H} \cdot g \cdot \boldsymbol{S} + \boldsymbol{S} \cdot A \cdot \boldsymbol{I} + \sum_{i=1}^{4} \boldsymbol{S} \cdot a_i \cdot \boldsymbol{I}_i, \quad (1)$$

where β is the Bohr magneton; g, the tensor of electronic Zeeman interaction; A, the tensor of magnetic hyperfine interaction between the electron of spin **S** and a nucleus of spin **I**; and a_i, the tensor of magnetic superhyperfine interaction between the electron of spin **S** and n equivalent nuclei of spin $\mathbf{I}_i$. In the case of axial symmetry of the g tensor:

$$\beta \cdot \boldsymbol{H} \cdot g \cdot \boldsymbol{S} = \beta\left[g_{\|} S_z H_z + g_{\perp}(S_x H_x + S_y H_y)\right], \quad (2)$$

where $g_{\mathrm{II}} = g_{zz}$, $g_{\perp} = g_{xx} = g_{yy}$, and g_{xx}, g_{yy}, g_{zz} are the principal values of the g tensor.

The RC (1) spectrum is described by the first and second terms; the RC (2) spectrum, by the first and third terms; and the RC (3) and RC (4) spectra, by the first term of the spin-Hamiltonian (1). The g, A, and a values for the radiation-induced paramagnetic centers in Bioglass obtained in the isotropic HF and SHF constant approximation are presented in the Table.

The observed hole centers in the glasses can be assigned to an ensemble of O^- centers, i.e., holes, trapped at non-bridging oxygen with different local environments. Basing on the presented EPR and literature data, we can to conclude that the RC (1) and RC (4) can be described in terms of HC_2 [23] and O^- [24] center models proposed for the alkali silicate glasses with high content of alkali modifiers. According to these models, the RC (4) is a hole captured at a Si–O tetrahedron which has 3 non-bridging oxygens and wave function of hole presumably being restricted strongly to the 3 non-bridging oxygens [23]. The RC (1) is the O^- center localized nearest to the Na^+ ion. It is the so-called L-center, ($Si–O^––Na^+$) [25], where the observed four-line hyperfine structure in the EPR spectrum is caused by one nucleus of the ^{23}Na isotope. Note that both RC (1) and RC (4) are characterized by high but slightly different thermal stability (see Table).

The RC (2) center can be interpreted as an electron trapped at oxygen vacancy. The SHF structure of the RC (2) centers could be explained by the interaction of the electron spin with four nearest ^{31}P nuclei of the glass structure. The RC (2) centers in Bioglass are characterized by high thermal stability and have no analogs in literature. The electron RC (3) centers are characterized by inhomogeneously broadened EPR line ($\Delta H_{pp} \cong 50$ G) and cannot be assigned to the well-known E' (Si) centers. The inhomogeneous broadening of the RC (3) EPR

Table. Spin Hamiltonian parameters obtained as the best fit of the experimental (T = 300 K) and simulated EPR spectra and thermal stability of the radiation-induced centers

Center number	Thermal stability	g values		A values		a values		Type of centers
		$g_\parallel$	$g_\perp$	$A_\parallel$, G	$A_\perp$, G	$a_\parallel$, G	$a_\perp$, G	
RC (1)	≤ 475 K	2.009 ± 0.001	2.005 ± 0.001	12 ± 1	12 ± 1	–	–	Hole
RC (2)	> 500 K	2.048 ± 0.001	2.048 ± 0.001	–	–	23 ± 2	23 ± 2	Hole
RC (3)	≤ 500 K	1.965 ± 0.005	1.953 ± 0.005	–	–	–	–	Electron
RC (4)	≤ 425 K	2.009 ± 0.001	2.005 ± 0.001	–	–	–	–	Hole

signal can be connected with presence of several volume and surface electron type centers with different local environments which give slightly shifted and statistically distributed g values, that form the observed EPR lineshape. The nature and structure of the RC (3) need additional study by EPR and other spectroscopic methods.

In conclusion, the ionizing UV-, X-, and γ-irradiation of bioactive glasses (Bioglass) at room temperature generates four types of stable paramagnetic centers that have been identified by EPR spectroscopy. The generation efficiency and type of radiation-induced paramagnetic centers depends heavily on the basic bioactive glass composition (i.e., ratio of the structure-forming elements to the modifiers) and is independent of the ionizing radiation kind and presence of Fe^{3+} non-controlled impurity. The spin Hamiltonian parameters and thermal stability for all radiation-induced centers in Bioglass have been evaluated. The RC (1) and RC (4) hole centers can be described in the frame of the HC_2 and O^- hole center models, respectively. The RC (1) is localized nearest to the ^{23}Na nucleus (L-center), whereas the RC (4) center is not related to any nucleus with magnetic momentum. The RC (2) can be interpreted as an electron trapped at oxygen vacancy. The RC (3) electron center cannot be assigned to the well-known E'(Si) centers and its nature needs additional study by different spectroscopic methods. The EPR data show good correlation with the thermo-stimulated luminescence (TSL) measurements. Particularly, the TSL glow peaks at 370–380 K, 420–430 K, and 690–710 K [15] can be assigned to the RC (4), RC (1), and RC (2), respectively. Pre-treatment of the samples in the 0.9 % NaCl solution and SBF results in formation of a surface coating of composition different from the basic Bioglass composition and influences the formation process of radiation-induced defects. Interaction of the physiological solution with surface artificial material is very complicated and it is not clear in every detail at present. Studies of surface coating composition and their influence on the formation process of the radiation-induced volume and surface defects in the bioactive glasses are in the progress.

Acknowledgement. This work has been supported financially by Grant BW/2003 of the Academy of Bydgoszcz.

References

1. L.L.Hench, R.J.Splinter, W.C.Allen, T.K.Greenlee, *J. Biomed. Mater. Res. Symp.*, **2**, 117 (1971).
2. L.L.Hench, E.C.Ethridge, Biomaterials, An Interfacial Approach, Acad. Press, New York (1982).
3. L.L.Hench, Materials in Clinical Applications, ed. P.Vincenzini (Techna, 1995), p.31.
4. T.Nakamura, Materials in Clinical Applications, ed. P.Vincenzini (Techna, 1995), p.35.
5. L.L.Hench, Summary and Future Directions, in: An Introduction to Bioceramics, eds. L.L.Hench, J.Wilson, World Scientific, Singapore (1993).
6. C.Y.Kim, A.E.Clark, L.L.Hench, *J. Non-Crystal. Sol.*, **113**, 195 (1989).
7. C.Ohtsuki, T.Kokubo, T.Tamamuro, *J. Non-Crystal. Sol.*, **143**, 84 (1992).
8. Y.Nakai, *Bull. Chem. Soc. Japan*, **38**, 1308 (1968).
9. A.Hasegawa, M.Miura, *Bull. Chem. Soc. Japan*, **40**, 2553 (1967).
10. R.A.Weeks, P.J.Bray, *J. Chem. Phys.*, **48**, 5 (1968).
11. M.Geoffroy, H.J.Tochon-Danguy, *Calcif. Tissue Int.*, **34**, S99 (1982).
12. Y.Doi, Y.Moriwaki, T.Aoba, M.Koni, *Calcif. Tissue Int.*, **34**, 547 (1982).
13. G.Bacquet, M.Sbit, M.Vignoles, G.Bonel, *Radiat. Effects*, **72**, 299 (1983).
14. P.Sharrock, G.Bonel, *Biomaterials*, **13**, 755 (1992).
15. B.Padlyak, S.Szarska, H.Jungner, *Opt. Appl.*, **XXX**, 709 (2000).
16. T.Kokubo, *J. Non-Crystal. Sol.*, **120**, 138 (1990).
17. L.Botter-Jensen, G.A.T.Duller, *Nuclear Tracks and Radiat. Measur.*, **20**, 549 (1992).

18. T.Jr.Castner, G.S.Newell, W.C.Holton, C.P.Slichter, *J. Chem. Phys.*, **32**, 668 (1960).
19. D.L.Griscom, *J. Non-Crystal. Sol.*, **40**, 211 (1980).
20. J.Kliava, EPR Spectroscopy of Disordered Solids, Zinatne, Riga (1988) [in Russian].
21. C.M.Brodbeck, R.R.Bukrey, *Phys. Rev. B*, **24**, 2334 (1981).
22. B.V.Padlyak, A.Gutsze, *Appl. Magn. Reson.*, **14**, 59 (1998).
23. J.W.H.Schreurs, *J. Chem. Phys.*, **47**, 818 (1967).
24. E.A.Zamotrinskaya, L.A.Torgashinova, V.F.Anufrienko, *Neorg. Mater.*, **8**, 1136 (1972).
25. A.N.Trukhin, *J. Non-Crystal. Sol.*, **123**, 250 (1990).

ЕПР-спектроскопія опромінених біологічно-активних стекол

Б.Падляк, С.Шарска

Досліджено ЕПР-спектри в Х-діапазоні ($\nu \cong 9.4$ ГГц) при температурах 77 і 300 К біологічно-активних (біологічних) стекол двох різних складів, опромінених УФ, рентгенівськими і γ-променями. Ефективність генерації центрів електронного і діркового типу суттєво залежить від основного складу біологічного скла і майже не залежить від виду іонізуючої радіації та присутності неконтрольованої домішки Fe^{3+} в структурі скла. Досліджено також вплив попередньої обробки у розчинах NaCl і модельної фізіологічної рідини на процеси формування радіаційних парамагнітних дефектів у біологічно-активних стеклах. Визначено параметри спін-гамільтоніана і термічну стабільність радіаційних центрів. Обговорюються електронна структура, особливості формування і можливі моделі радіаційних парамагнітних центрів у структурі біологічного скла.